Surface Wind over Tropical Oceans: Diagnosis of the Momentum Balance, and Modeling the Linear Friction Coefficient

John C. H. Chiang

Lamont-Doherty Earth Observatory, Columbia University, Palisades, New York

Stephen E. Zebiak

International Research Institute for Climate Prediction, Lamont-Doherty Earth Observatory, Columbia University, Palisades, New York

(Manuscript received 30 November 1998, in final form 9 July 1999)

ABSTRACT

Previous diagnostic studies of surface wind momentum balances over tropical oceans showed that, under a linear friction assumption, the meridional friction coefficient is two to three times larger than the zonal friction coefficient, and that both friction coefficients exhibit a pronounced meridional dependence. The authors' diagnosis of a global marine surface dataset confirms these results. Furthermore, it is shown that to first approximation the friction coefficients are independent of longitude and season in the tropical band between ~20°S and ~20°N. Poleward of 20°N and 20°S, the coefficients are no longer solely a function of latitude. To explain these empirical results, a simple analytical model of the friction coefficient is formulated based on the simplest *K*-theory mixed-layer parameterization, assuming constant viscosity. The model does a good job of reproducing the observed zonal friction coefficient, but does poorly for meridional friction. The poor result is thought to be from model sensitivity to the specified planetary boundary layer (PBL) thickness. By reversing the calculation, using observed meridional friction coefficients, and assuming no meridional winds at PBL top, model PBL heights were derived that compared favorably with zonally averaged inversion heights for June–August over the tropical Atlantic.

This model suggests that both coefficients increase away from the equator because of the decrease in PBL thickness. Furthermore, the zonal friction coefficient is smaller than the meridional coefficient because strong zonal winds at the top of the boundary layer mixes down, reducing the retarding influence of surface zonal momentum fluxes. The results also suggest that the boundary layer top winds and height are important components in modeling surface winds over the tropical oceans.

1. Introduction

The three-way steady momentum balance between the Coriolis term, the pressure gradient term, and the frictional term is widely used as the simplest conceptual and quantitative model for monthly mean surface wind. It has been shown in numerous observational studies to be widely applicable for surface wind over tropical oceans (Murphree and van den Dool 1988; Zebiak 1990; Deser 1993; Li and Wang 1994). The nonlinear advection terms have been shown to play only a minor role in the balance and only in limited regions over the tropical oceans. Deser (1993) showed in particular for the tropical Pacific that inclusion of the nonlinear terms improved the zonal wind simulation in limited regions of the northeast trades, equatorial easterlies, and off of South America. Stout and Young (1983) showed the acceleration terms to be significant over the southwest monsoon flow over the tropical Indian Ocean.

The form of parameterization of the frictional term has been shown to be of fundamental importance to this balance. The linear ''Raleigh'' parameterization with the same damping coefficient for both zonal (u) and meridional (v) wind had been used for most diagnostic studies of surface wind, and for the simplest models of tropical circulation. However, Deser (1993) showed in a diagnostic study over the tropical Pacific Ocean that the damping timescale for the meridional wind is in fact two to three times shorter than the damping time for zonal wind. Subsequent studies by Li and Wang (1994) and Kushnir and Kaplan (1994) showed a systematic meridional dependence in the magnitude of the frictional coefficients within the Tropics; in general, the magnitude of the coefficients increases approximately symmetrically away from the equator. From equator to 15°N/S, the zonal coefficient increases by roughly a factor of 2, and the meridional component by about a factor of 1.5. Furthermore, the value of the u coefficient

Corresponding author address: Mr. John C. Chiang, Lamont-Doherty Earth Observatory, Columbia University, Palisades, NY 10964.
E-mail: jchiang@ldeo.columbia.edu

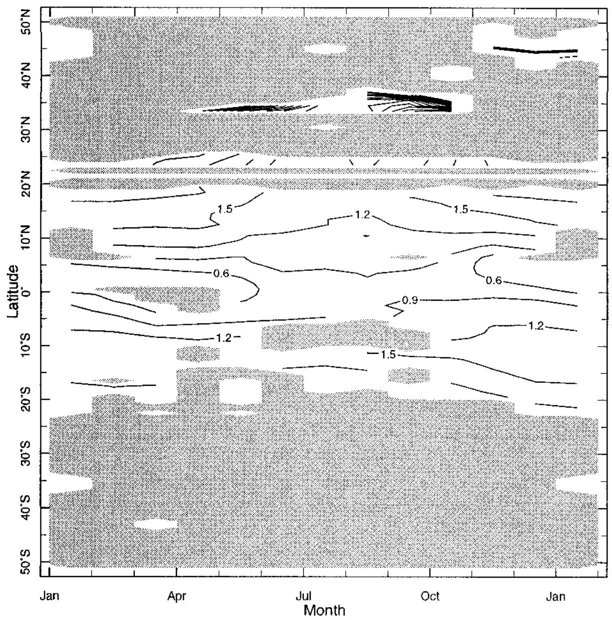

FIG. 1. The u friction coefficient ($\times 10^{-5}$ s^{-1}) as a function of latitude and month. Regression values are masked out if the associated correlation magnitude is below 0.45.

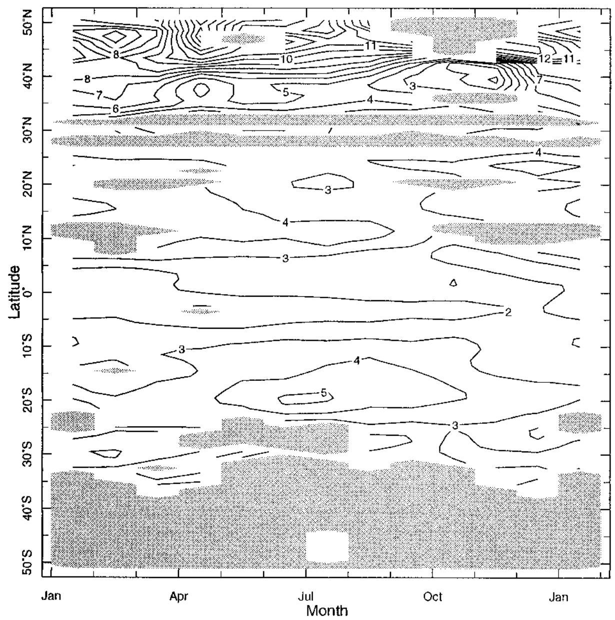

FIG. 2. Same as Fig. 1 but for the v friction coefficient.

was found to be smaller than the v coefficient at the same latitude.

Deser (1993) argued that the different damping timescales of the u and v coefficients are a result of the different vertical profiles of u and v in the planetary boundary layer (PBL). Specifically, while the zonal wind generally increases from the surface to the top of the boundary layer, the meridional wind generally decreases to a small or zero magnitude at the top of the PBL. This implies that the curvature of the vertical profile for u is smaller than that for v near the surface, which by flux-gradient theory implies a stronger frictional retardation for v. Kushnir and Kaplan (1994) supported Deser's explanation in a GCM setting, by computing the linear momentum balance of surface wind and pressures from GCM output, but also taking into account the influence of winds from the model layer nearest the surface.

The purpose of this paper is twofold. 1) To refine and extend the previous quantification of the linear friction coefficients—in particular, to define the limits of applicability of a purely meridionally varying friction coefficient; and 2) to model the qualitative features of the friction coefficient, starting off from Deser's suggestion of a physical mechanism. From our results we suggest a simple physical explanation for the observed behavior of the u and v friction coefficients, and why they differ in magnitude.

The paper is organized as follows. Section 2 contains our quantification of the linear friction coefficients. Section 3 contains the model formulation, and its application using reanalysis data. In section 4 we invert our model in an interesting computation to determine approximate PBL heights using observed v friction coefficients. We summarize and discuss our results in section 5.

2. Diagnosis of the momentum balance

a. Preliminaries

The equations for steady surface linear momentum balance can be written as

$$-fv + \frac{1}{\rho}\frac{\partial p}{\partial x} = -\alpha_u u \tag{1a}$$

$$fu + \frac{1}{\rho}\frac{\partial p}{\partial y} = -\alpha_v v, \tag{1b}$$

where u, v are the zonal and meridional wind components, respectively; ρ is air density, and p the pressure. Here α_u and α_v are friction coefficients for u and v, respectively. In the most general instance we assume them to be functions of x, y, and time. In keeping with the results of previous studies, we neglect the advection term in the balances.

Figures 1 and 2 show our computation for the u and v friction coefficients, respectively, as a function of latitude and month. They are computed over all ocean grid points, utilizing monthly climatological winds, pressure, and air density data from Da Silva et al. (1994). The Da Silva dataset has 1° lat × 1° long resolution. The friction coefficients were calculated for each latitude and month by regressing the departure from geostrophy [i.e., the lhs of Eq. (1)] with the appropriate wind component. For example, Fig. 3 shows for July at 10.5°N the [fu

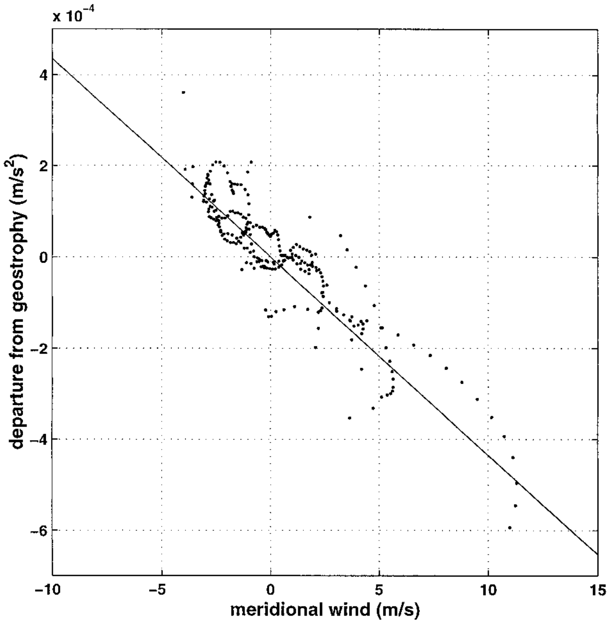

FIG. 3. Scatterplot of the [$fu + (1/\rho)(\partial p/\partial y)$] term against v, for Jul at 10.5°N. The line is regression of [$fu + (1/\rho)(\partial p/\partial y)$] on v, constrained to pass through the origin: $\alpha_v = 4.35 \times 10^{-5}$ s^{-1}.

$+ (1/\rho)(\partial p/\partial y)$] term plotted against v, for each longitude gridpoint. The line shown is the least-squares regression of the departure from geostrophy on meridional wind, constrained to pass through the origin [as required by the form of Eq. (1)]. The negative of the slope is the estimate for α_v. This method is in keeping with Kushnir and Kaplan, but unlike Li and Wang, who compute friction coefficients directly at each grid point and then applies a zonal average. As a rough measure of significance, we computed correlation coefficients for each regression, masking out in Figs. 1 and 2 those friction coefficients whose r-value were below 0.45 (low values of correlation imply that the regression values are meaningless). Note that there is spatial autocorrelation in the data (e.g., this is evident from the structure of the scatterplot in Fig. 3), which needs to be taken into account when assessing significance. Correlations above 0.45 are significant at the 0.05 level using a 1 tail t test, assuming a spatial decorrelation length of 20°, and each zonal band having about 240 data points.

Our results show that the u friction coefficient is two to three times less than the v coefficient, and that both coefficients increase symmetrically about the equator, up to about 20°S and 20°N. This is in agreement with the results of Li and Wang (1994) and Kushnir and Kaplan (1994). Neither the u or v friction coefficient equatorward of 20°S and 20°N exhibit strong seasonal dependence, suggesting that to first approximation the coefficients are independent of the season. Poleward of 30°N, the v friction coefficient contours show sharp latitudinal and temporal gradients. This suggests the inadequacy of linear friction in parameterizing the missing physics in the linear momentum balance (1) for the midlatitudes. Specifically, we know that transient eddies are important poleward of the Tropics, and our results may reflect the importance of nonlinear transient terms in the steady momentum balance. Murphree and van den Dool (1988) found from analysis of the January 1987 NMC 1000-mb analysis that transient eddies is a significant part of the surface momentum balance for latitudes poleward of about 15°S and 15°N.

In general, the correlation is higher in the Tropics, and lower in the midlatitudes. It is possible that low correlation is due to a lack of zonal variation in the variables that are being compared. For such cases, errors may dominate the variance, and the correlation may suffer as a result. However, we checked for such effects, and found that at no latitude can any of the variables be considered to lack variance relative to any other latitude. We conclude that while errors may influence the outcome of the correlation, there is enough zonal variation at all latitudes to claim that the correlations point to significant differences in the steady momentum balance between the tropical (high correlation) and extratropical (generally low correlation) regimes.

b. Time-independent friction coefficients

The lack of significant seasonal variation in the friction coefficients suggests that it is physically meaningful to compute time-independent coefficients. We recomputed the friction coefficients by taking the regression over all months over a latitude band. The values of these coefficients (and associated correlation) are shown in Fig. 4. The correlations for both the u and v friction regressions are high in the Tropics (18°N–18°S), although the correlation for v is higher than that for u. The correlation drops significantly for both regressions poleward of this latitude band.

Does the inclusion of nonlinear advection terms affect the friction coefficients? We recomputed the friction terms, but with the nonlinear terms [$u(\partial u/\partial x) + v(\partial u/\partial y)$] added to the lhs of Eq. (1a), and [$u(\partial v/\partial x) + v(\partial v/\partial y)$] added to the lhs of Eq. (1b). The results (not shown) indicate that these friction coefficients vary little from Fig. 4, consistent with previous studies that show the minor role played by nonlinear terms in the balance.

How reproducible are these friction coefficients in analysis datasets? We compute friction coefficients from the National Centers for Environmental Prediction (NCEP; Kalnay et al. 1996) reanalysis 1000-mb winds (Fig. 5). The qualitative features—$\alpha_u < \alpha_v$, and the increase from the equatorial region to higher latitudes, and the larger increase for α_v than for α_u—are also exhibited by the NCEP coefficients. While the details of NCEP α_u are similar to those of Da Silva, NCEP and Da Silva α_v differ: NCEP α_v is approximately uniformly

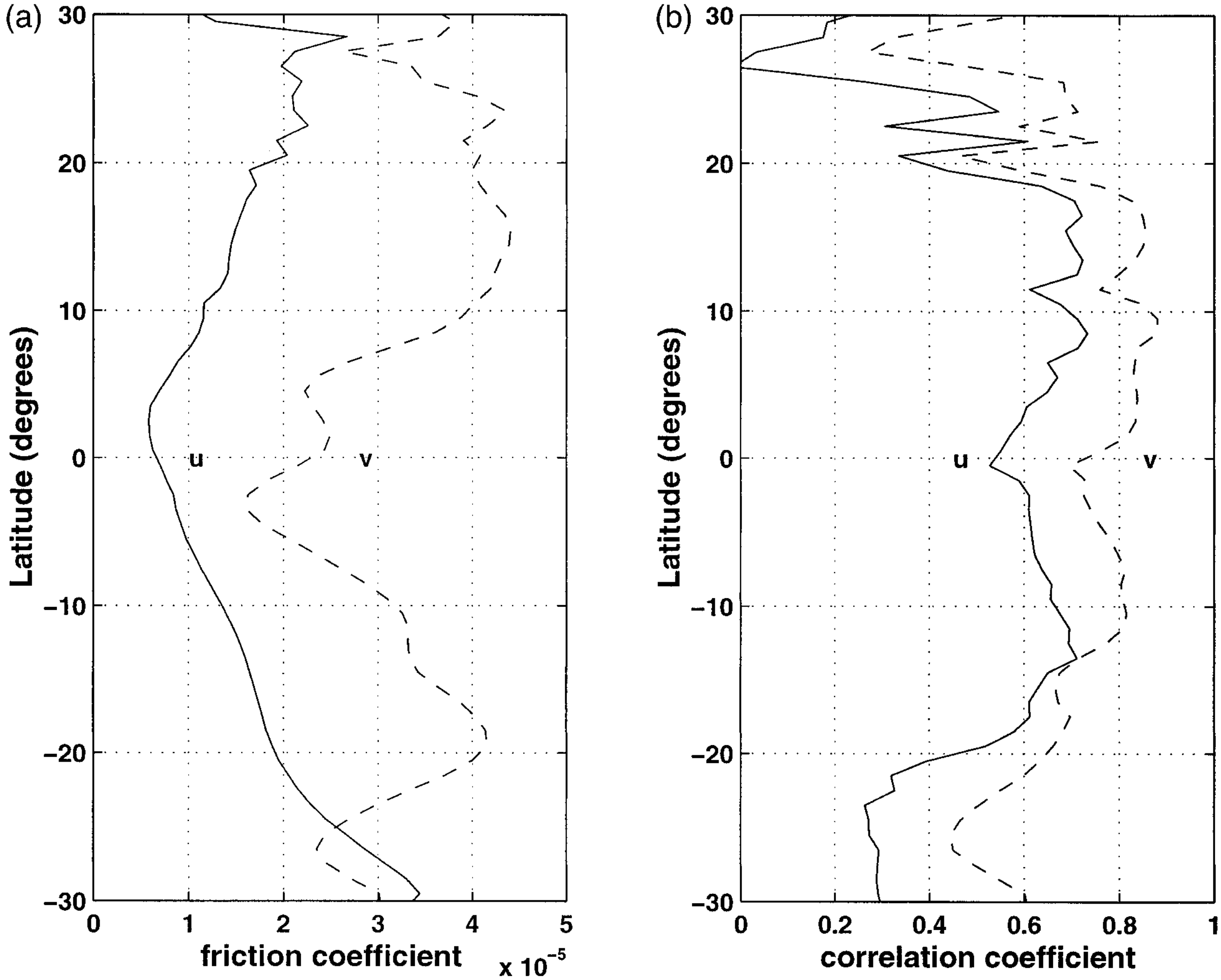

FIG. 4. (a) The u (solid line) and v (dashed line) friction coefficients as a function of latitude, from regression over all zonal and time points. Coefficient units are s^{-1}. (b) Correlation coefficients associated with the regression in (a).

weaker than Da Silva α_v by about 1×10^{-5} s^{-1}. Also, NCEP α_v does not show as much structure near the equator. The correlation is different as well: correlation coefficients for NCEP are at the same high level for both α_u and α_v (between 0.6 and 0.9), and only the α_u correlation poleward of 20°S decreases significantly.

The coefficients derived by Kushnir and Kaplan (1994) using European Centre for Medium-Range Weather Forecasts (ECMWF) analysis for December, January, and February 1980–89 is similar to the NCEP coefficients, but does show a little bit of structure near the equator for α_v.

In summary, the details of the friction coefficients in analysis datasets differ from that of Da Silva. In particular, the NCEP α_v is smaller by about 1×10^{-5} s^{-1} compared to Da Silva's α_v; this indicates that the surface v momentum balance in the reanalysis may be deficient. However, the qualitative features of the friction coefficients are robust; namely, between 20°N and 20°S:

- $\alpha_u < \alpha_v$ at each latitude point,
- both friction coefficients increase away from the equator by approximately a factor of 2 from the equator to ~20°N and ~20°S,
- α_v increases faster than α_u.

3. Modeling the friction coefficients

We demonstrate that a simple Ekman boundary layer model is capable of explaining the qualitative behavior of the friction coefficients. We first justify in subsection (a) the choice of using the simplest Ekman layer formulation for this problem. In (b) we manipulate the boundary layer model to obtain an analytical expression for the friction coefficients. We quantify and interpret our model in (c), and test the model with NCEP reanalysis data (d).

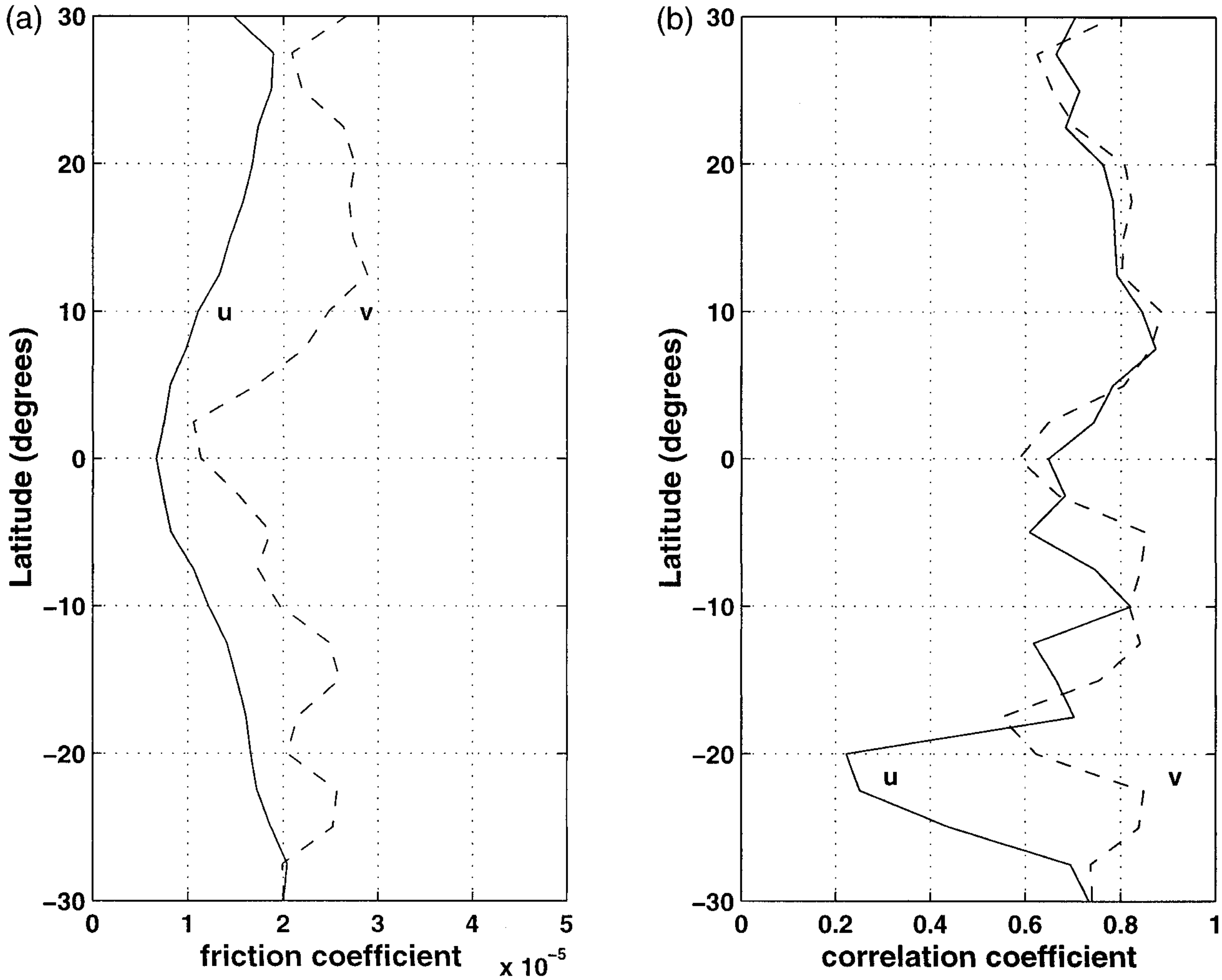

FIG. 5. Same as for Fig. 4 but using NCEP reanalysis 1000-mb data.

a. Motivation for the choice of model

Deser (1993) used *K*-theory, that is,

$$\mathbf{F} = \frac{1}{\rho}\frac{\partial}{\partial z}\left(\rho K\frac{\partial \mathbf{V}}{\partial z}\right) \tag{2}$$

(K is the eddy viscosity, and ρ the density) as the basis for her qualitative explanation of why $\alpha_u < \alpha_v$. The model itself does not contain the asymmetry in the horizontal, which is required to explain the different magnitudes of α_u and α_v. Rather, the crux of Deser's explanation comes from exploiting an asymmetry of the large-scale tropical circulation: that meridional winds at PBL top are generally small relative to surface meridional winds, whereas zonal winds at PBL top are generally much larger and in the same direction as surface zonal winds. We will use this model (*K*-theory, constant coefficient) as the basis for our own analysis, for the following reasons. First, consider the nature of the surface marine data. There is uncertainty in the representative height of the surface wind observations, because of the different ways that surface wind is reported (Beaufort scale or direct measurements), and the different heights of ship anemometers (Cardone et al. 1990). This is a big problem since typically there is strong vertical wind shear in the surface layer. The typical vertical length scale in the surface layer is much smaller than common ship height (at most 0.1 m, as opposed to meters or tens of meters). Hence, it is appropriate to view the observed winds as representative of winds in the upper portion of the surface layer, and a lower boundary condition for the Ekman-layer wind profile. Since the data is monthly climatology, we need to consider time-mean models. Hence, a steady-state Ekman-layer model is a suitable starting point.

We choose the simplest *K*-theory with constant viscosity because of the limited information on winds above the surface; we require a model with as few degrees of freedom as possible in order to constrain it. Deser's (1993) experience suggests that the simplest *K*-theory model is appropriate for this purpose. As we will show, this simplified model is well capable of explaining the qualitative behavior of the friction coefficients.

b. Model formulation

For convenience, we switch to a pressure vertical coordinate:

$$\begin{aligned} v\frac{\partial^2 u}{\partial p^2} &= -f\upsilon + \frac{\partial \phi}{\partial x} \\ v\frac{\partial^2 \upsilon}{\partial p^2} &= fu + \frac{\partial \phi}{\partial y}, \end{aligned} \tag{3}$$

where ϕ is the geopotential, and v is the constant eddy viscosity coefficient. Assuming the standard mixing length hypothesis with a typical mixing length ~30 m and boundary layer shear $\sim 5 \times 10^{-3}$ s^{-1} gives an eddy viscosity $K \sim 4.5$ m^2 s^{-1}. However, dependence on shear implies a fairly large range for K: up to 30 m^2 s^{-2} for monsoonal flows (Young 1987). We choose a value of $v = 650$ Pa^2 s^{-1} (~ 6.5 m^2 s^{-1}); this choice of v gives friction coefficients comparable to observed values, though we made little effort toward tuning.

We interpret the model winds at the "surface" ($p = p_0$) to be representative of the winds on the upper part of the surface layer. We cannot apply the classical Ekman spiral solution, since pressure gradients are not independent of height in the Tropics, and geostrophy does not hold for the free atmosphere near the equator. Instead, we follow the approach of Neelin (1988) by decomposing the problem using vertical modes of the diffusion operator. Its eigenfunctions can be written as

$$a_j \cos\left(m_j \frac{p - p_T}{\Delta p}\right) + b_j \sin\left(m_j \frac{p - p_T}{\Delta p}\right), \tag{4}$$

where $j = 0, 1, 2, 3, \ldots$; p_0 and p_T are the pressures at the surface and top of the boundary layer, respectively; $\Delta p = p_0 - p_T$ is the thickness of the boundary layer; and m_j are the eigenvalues. At the surface ($p = p_0$) we apply a linearized form of the bulk formula surface momentum flux:

$$-\frac{\partial \mathbf{V}}{\partial p}(p_0) = c\mathbf{V}(p_0). \tag{5}$$

The coefficient c is taken to be 1.5×10^{-4} Pa^{-1}, from bulk parameterization estimates of surface momentum fluxes assuming a drag coefficient $C_D \sim 1.2 \times 10^{-3}$ and mean wind speed ~6.5 m s^{-1}. Climatological wind speeds range from 5 to 8 m s^{-1} over tropical oceans, so the estimate of c is good to ~30%, assuming that the bulk of the error in c comes from specified wind speed. At the top of the boundary layer we use a flux-ratio approach, which assumes a constant ratio between flux at the top and at the surface (Stull 1988):

$$\frac{\partial \mathbf{V}}{\partial p}(p_T) = A_R c\mathbf{V}(p_0). \tag{6}$$

There is little in the way of empirical results to guide us on the value of A_R, other than the reasonable assumption that boundary layer top flux is a small fraction of the surface flux. We use $A_R = 0.2$, implying that 20% of the surface momentum flux escapes through the top of the PBL. The alternative that is commonly applied—no flux at the top ($A_R = 0$)—is problematic under the assumption of a flux gradient parameterization with fixed viscosity, as the wind shear vanishes at the top. Measurements of the wind profile over the tropical ocean PBL shows that this is generally not the case. We add, however, that our conclusions in this paper remain unchanged whether we choose $A_R = 0.2$ or $A_R = 0$, implying insensitivity of our analysis to the numerical choice of the flux ratio.

Applying boundary conditions (5) and (6) using the eigenfunction (4) gives us two equations, one relating b_j to a_j (7), and the other determining the eigenvalues m_j:

$$b_j = a_j \frac{\cos(m_j)}{\dfrac{m_j}{A_R c\Delta p} - \sin(m_j)}, \tag{7}$$

$$\frac{m_j}{c\Delta p}\sin(m_j) = A_R + \cos(m_j). \tag{8}$$

The boundary layer thickness Δp is a parameter in our model. Note that the eigenvalues m_j (and consequently the eigenvectors) are functions of the boundary layer thickness.

Figure 6 shows the form of the eigenfunctions for $j = 0$–4 assuming a boundary layer depth of 150 mb. The number of nodes (where the function equals zero) equals the eigenfunction number. As the vertical structure of climatological winds in the tropical PBL is not complicated, it is plausible to model the vertical structure using only the first few eigenfunctions. Figure 7a shows vertical structures obtained by combining the first two ($j = 0, 1$) eigenvectors in various proportions. They appear to cover a range of profiles commonly seen in the PBL. For example, the $R = -0.15$ or -0.3 profile (where R is the ratio of the amplitude of the $j = 1$ eigenvector to the $j = 0$ eigenvector) resembles the zonal wind profile measured during ATEX (Fig. 7b; Augstein et al. 1973), whereas $R = -1$ resembles that for υ.

Motivated by this observation, we make the simplifying assumption of truncating the vertical expansion to just the $j = 0$ and $j = 1$ modes (this is equivalent to keeping the mean and the mean shear components only). This is not just a step to obtain analytical solutions. It is necessary to reduce the vertical degrees of freedom to two, since there are only two pieces of information to constrain the vertical profile of wind: the surface value, and the value at the top of the PBL. Given the limited data, the two modes chosen represent our best estimate for the vertical wind profile.

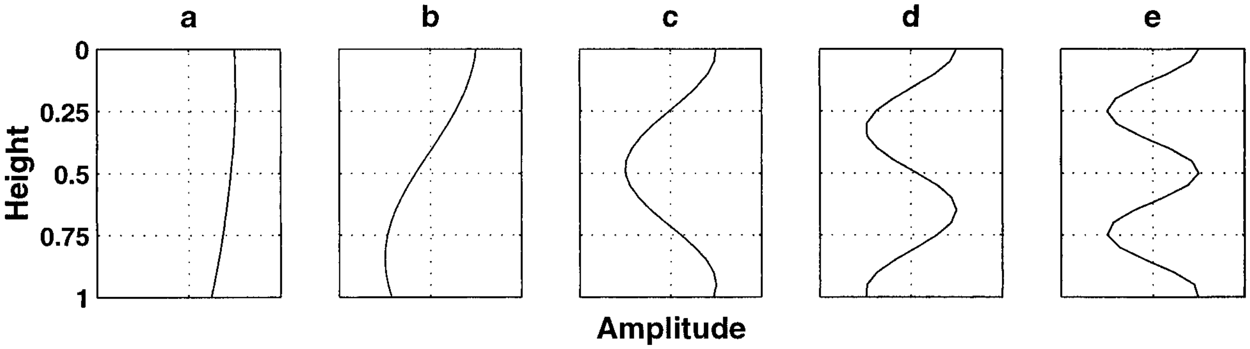

FIG. 6. The first five eigenvectors of the diffusion operator. The first one from the left is the $j = 0$ mode, and the second one is the $j = 1$ mode. The height coordinate is $(p - p_T)/\Delta p$, where p_T is the boundary layer top and Δp is the PBL thickness.

Expanding u, v, and ϕ in terms of the truncated normal modes

$$[u, v, \phi] \cong \sum_{j=0}^{1} [u_j, v_j, \phi_j]A_j(p), \qquad (9)$$

where $A_j(p)$ is the vertical profile of the jth mode:

$$A_j(p) = \cos\left(m_j\frac{p - p_T}{\Delta p}\right) + A_R c\Delta p \frac{\cos(m_j)\sin\left(m_j\dfrac{p - p_T}{\Delta p}\right)}{m_j - A_R c\Delta p \sin(m_j)} \qquad (10)$$

and substituting them into our steady-state momentum equations, (3) gives:

$$-\nu\frac{u_j A_j m_j^2}{\Delta p^2} = -f v_j A_j + \frac{\partial\phi_j}{\partial x}A_j \qquad j = 0, 1$$
$$-\nu\frac{v_j A_j m_j^2}{\Delta p^2} = f u_j A_j + \frac{\partial\phi_j}{\partial y}A_j. \qquad (11)$$

Adding the $j = 0$ and $j = 1$ equations, and projecting the equations to the surface ($p = p_0$) with a little rearranging leads us to

$$\alpha_u u - f v + \frac{\partial\phi}{\partial x} = 0$$
$$\alpha_v v + f u + \frac{\partial\phi}{\partial y} = 0, \qquad (12)$$

where u, v, and ϕ are the values of zonal wind, meridional wind, and geopotential at $p = p_0$, obtained under the assumption that the full winds can be modeled by just the two vertical components. The friction coefficients α_u and α_v are given by:

$$\alpha_{u,v} = \frac{\nu}{\Delta p^2}\frac{m_0^2 + R_{u,v}\dfrac{A_1(p_0)}{A_0(p_0)}m_1^2}{1 + R_{u,v}\dfrac{A_1(p_0)}{A_0(p_0)}}, \qquad (13)$$

where $R_{u,v}$ is the ratio of amplitude of the $j = 1$ mode to the $j = 0$ mode, and can be found from values of the wind components at the surface and top of the PBL:

$$R_u = -\frac{u(p_0) - u(p_T)A_0(p_0)}{u(p_0) - u(p_T)A_1(p_0)} \qquad (14)$$

(similarly for R_v). Note that $R_{u,v}$ depends on the winds, which in turn depends on $\alpha_{u,v}$, etc. . . . , so the formulation is nonlinear.

c. Quantifying and interpreting the model

Figure 8a shows α as a function of R and PBL thickness, calculated with $\nu = 650$ Pa^2 s^{-1} and $c = 1.5 \times 10^{-4}$ Pa^{-1}. Only the positive values of the contours are shown, and the shaded region indicates where friction coefficients are negative. For typical profiles of boundary layer winds (R ranging from -2 to 0) the ranges of the friction coefficient are certainly within the correct order of magnitude. Note the strong dependence of friction on the boundary layer thickness. For positive values, the friction coefficient increases as boundary layer thickness decreases.

Negative coefficients occur when $[-m_0^2 A_0(p_0)/m_1^2 A_1(p_0)] < R < [A_0(p_0)/A_1(p_0)]$, corresponding to the physical situation where winds at the top of the PBL are much stronger and of the same sign as winds at the surface (e.g., see the $R = 0.3$ profile in Fig. 7b). In this case, stronger winds above the surface mixes down, counteracting the retarding fluxes from the surface sufficiently so that the net influence of the turbulent transfer is to accelerate the surface flow in the same direction. This may not be an uncommon situation. For example, northward-moving cross equatorial trades just north of the cold tongue in the eastern equatorial Pacific is thought to be accelerated by momentum mixing from strong southerlies aloft (Wallace et al. 1989). This momentum mixing is set up by the sudden transition from a stable to unstable PBL, as air parcels moved from the cold tongue region into much warmer waters of the North Equatorial Countercurrent. Li and Wang (1994) show, in their Fig. 3, regions of the tropical Pacific

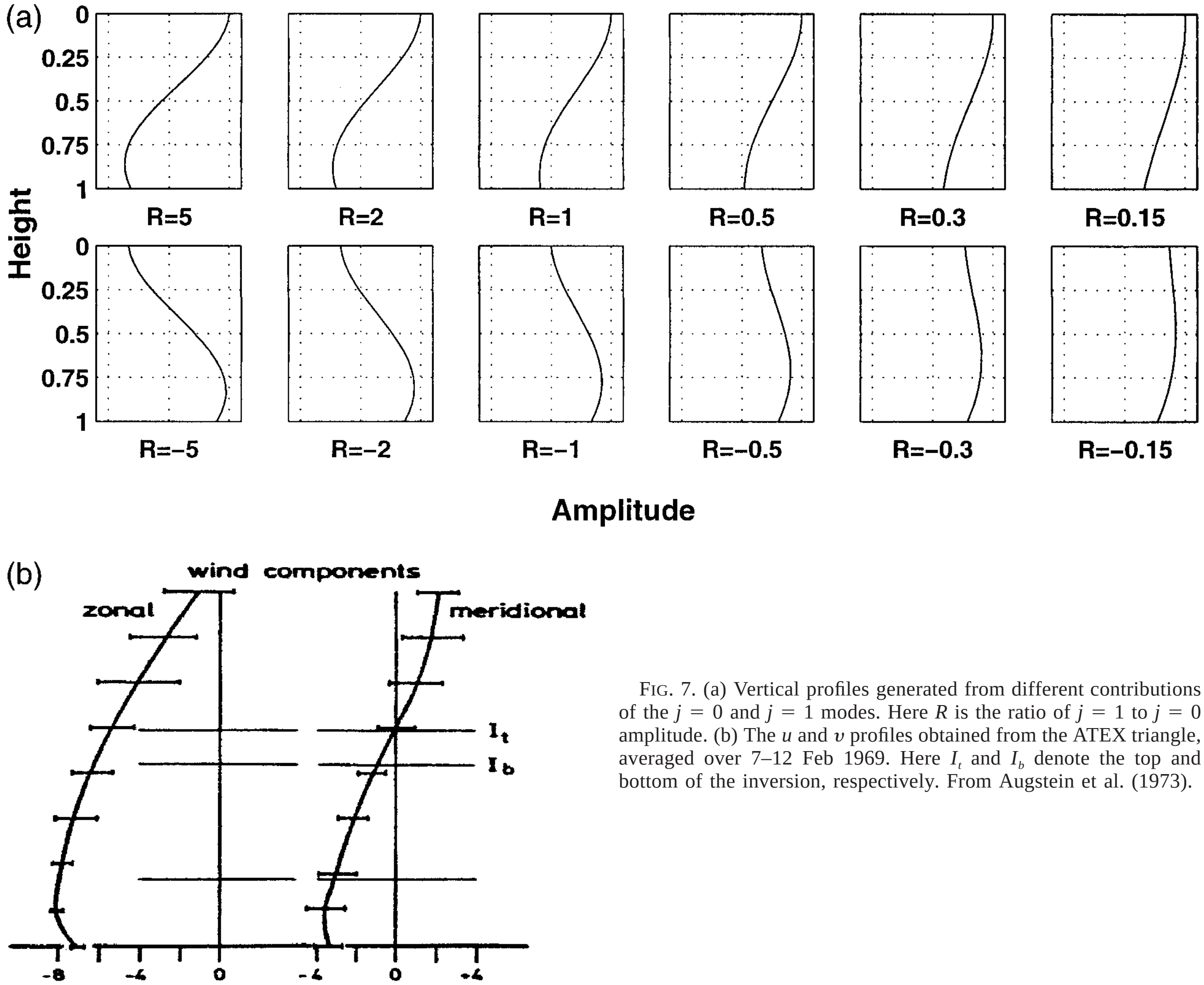

FIG. 7. (a) Vertical profiles generated from different contributions of the $j = 0$ and $j = 1$ modes. Here R is the ratio of $j = 1$ to $j = 0$ amplitude. (b) The u and v profiles obtained from the ATEX triangle, averaged over 7–12 Feb 1969. Here I_t and I_b denote the top and bottom of the inversion, respectively. From Augstein et al. (1973).

where the friction coefficient is negative. Parts, though not all, of the eastern equatorial Pacific north of the cold tongue was identified as regions of negative meridional friction coefficient. It was, however, unambiguously identified as a region of negative zonal friction coefficient.

The coefficients become positive again when $R > [A_0(p_0)/A_1(p_0)]$. This transition occurs when the wind at the surface changes sign from positive (same sign as the top PBL winds) to negative—compare the $R = 0.3$ profile to the $R = 1$ profile, for example. Equation (13) also predicts that the v frictional coefficient is typically larger than the u frictional coefficient. Taking $R = -1$ as a typical v wind profile, and $R = -0.15$ as a typical u wind profile (Fig. 8b), the ratio α_v/α_u is between 2 and 3 for thickness between 75 and 275 mb (Fig. 8c). This is consistent with the observed ratios as reported by Deser (1993) and others. Clearly the observed ratios are sensitive to the exact nature of the vertical wind profile, so we do not claim such a precise match. However, given typical profiles for u and v, our model does predict larger v friction coefficients.

Note also our model prediction that the rate of change of friction with boundary layer thickness depends on the vertical wind profile. This is readily seen in Fig. 8b, where the coefficient for the $R = -1$ profile (typical of v) changes more rapidly than the coefficient for the $R = -0.15$ profile (typical of u) as boundary layer thickness changes. As we discuss in section 5b, we suggest this as the reason why the observed v friction coefficient increases more rapidly with latitude than the u friction coefficient.

d. Obtaining friction coefficients from reanalysis data

To obtain friction coefficients from (13), PBL heights and winds at the top of the PBL are needed. These are not usually available from observations for any length of time for any substantial region [although PBL top winds may be inferred from satellite cloud drift data—

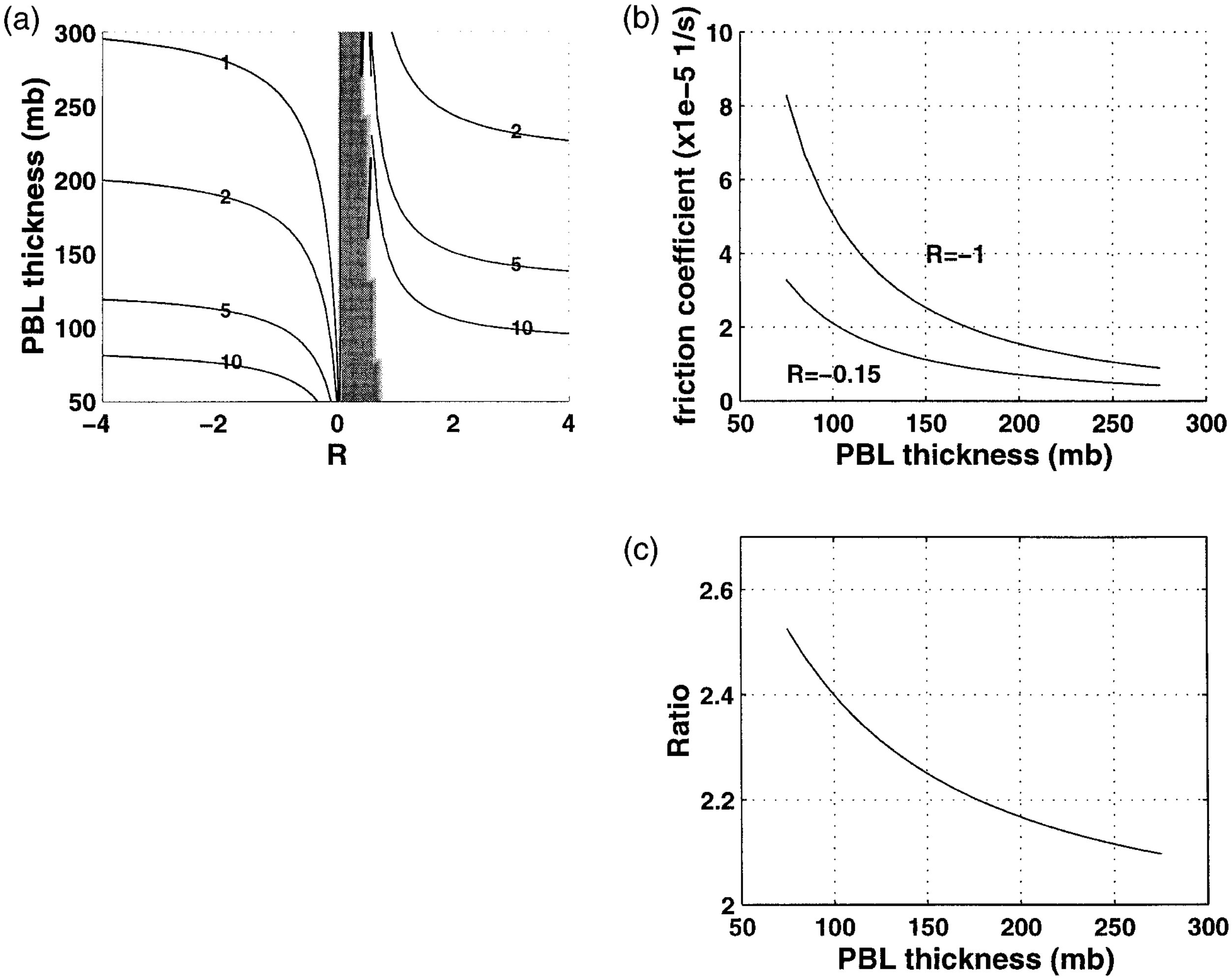

FIG. 8. (a) Contours of friction coefficients as a function of R and PBL thickness. Contour values are in 10^{-5} s^{-1}, and the negative coefficient region is shaded. (b) Friction coefficients as function of PBL thickness for two values of R, corresponding to typical v ($R = -1$) and u ($R = -0.15$) profiles. (c) Ratio ($R = -1 : R = -0.15$) of the two curves shown in (b).

the Monsoon Experiment (MONEX; Young 1987) being a good example]. We therefore rely on NCEP reanalysis to obtain PBL top winds.

In interpreting what the PBL depth is, note that there are two height scales for the mixed layer. For a neutral barotropic layer, the Ekman depth $(v/f)^{1/2}$ is the correct scale height. However, for the nonneutral boundary layer, the scale height is more likely set by thermal convection within the PBL, especially in unstable situations. Deardorff (1972) suggests that the inversion height (more accurately, the inversion base) is a more appropriate scale height for the PBL. We will return to this issue later (section 4a), but for now we will assume inversion height as the proper height scale.

It is well known that the inversion height varies significantly over the tropical oceans, from 900 mb and lower off the coast of California to 800 mb or higher in the trade wind region. However, the detailed structure of the tropical Pacific inversion height is not known. There have been attempts to estimate it using low cloud-top temperature from satellite data and the assumption of a constant lapse rate (Minnis et al. 1992; Betts et al. 1992; S. Esbensen 1997, personal communication). We apply the same technique to compute inversion heights, using low cloud-top temperatures from the International Satellite Cloud Climatology Project (ISCCP) D2 dataset (Rossow et al. 1996), 2-m air temperatures from NCEP, and a constant lapse rate of 5.2 K km^{-1}. The choice of the lapse rate was determined by regressing observed values of average inversion height reported in various literature sources (Riehl et al. 1951; Gutnick 1958; Holland and Rasmussen 1973; Augstein et al. 1974; Chertock et al. 1993; Schubert et al. 1995; Kloesel and Albrecht 1989), against the difference between the surface air temperature and the low cloud-top temperature, at the locations where the inversion heights are reported.

While there is good reason to believe that low cloud-top height correlates well with inversion height, there

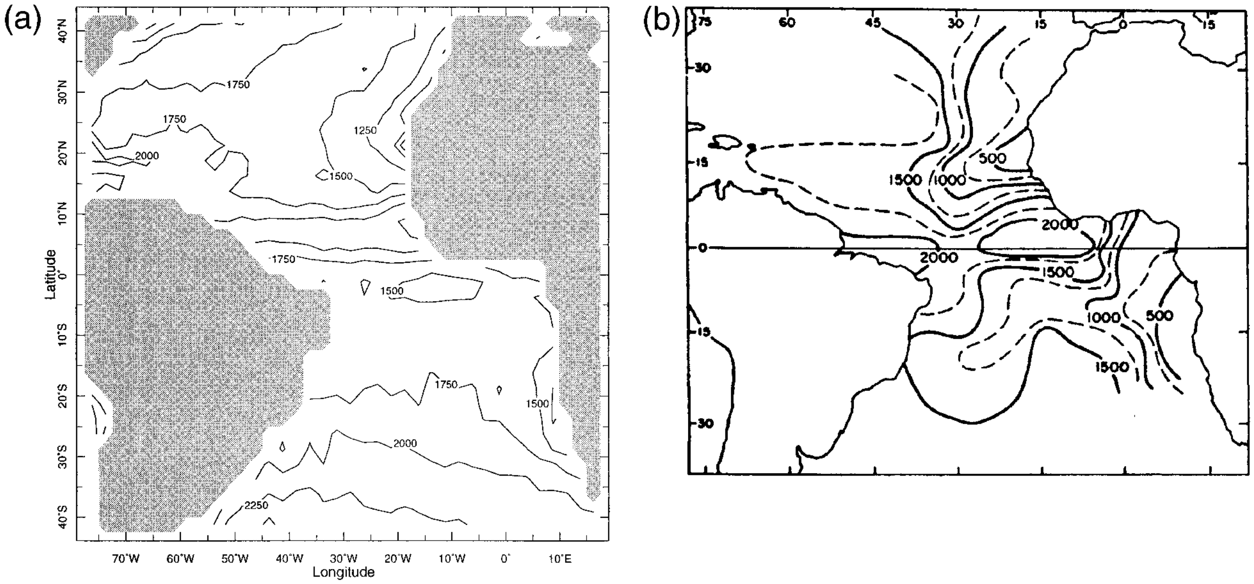

FIG. 9. (a) PBL height over the tropical Atlantic Jun–Aug derived from ISCCP D2 low cloud-top temperatures (1989–91), assuming a 5.2 K km^{-1} lapse rate. The contour values are in m. (b) Inversion heights over the tropical Atlantic from measurements made by the *Meteor* expedition (von Ficker 1936).

are enough uncertainties in the measurement of the low cloud-top temperature, as well as uncertainties in the choice of lapse rate, to be unsure of the outcome of such a calculation. However, we and others (S. Esbensen 1997, personal communication) find that the heights generated by this procedure compare surprisingly well with fragmentary observations of PBL height. For example, Fig. 9 shows the derived inversion heights over the tropical Atlantic averaged over June–August, compared with an observed map of inversion height over the same area (von Ficker 1936). The von Ficker map, derived from kite sounding data collected during the 1925–27 expedition of the German R/V *Meteor I*, can be regarded as typical of the northern summer (Schubert et al. 1995). The derived inversion heights seem to capture the east–west structure in the subtropical latitudes, although the heights over the west coasts of northwest and southwest Africa are too high. The height over the equatorial region corresponds well in magnitude, although the 2000-m contours (over the location of the ITCZ) are farther north than what is seen in von Fickers' map. Despite significant differences, the inversion height inferred through low cloud-top temperatures is at least qualitatively correct. One of the reviewers pointed out the resemblance between our derived height structure and the structure of the June–August lower-tropospheric static stability as given in Klein and Hartmann (1993), keeping in mind the observed negative correlation between inversion strength and inversion height (Hastenrath 1991).

We calculate α from the zonally averaged momentum balance version of (13) and (14), which can easily be shown to be the same equations except that R_u and R_v are computed from the zonally averaged winds at the surface and top of the PBL. The values of the climatological winds at the surface and PBL top used in this calculation are obtained from NCEP reanalysis data (winds at the PBL top are obtained by linearly interpolating between grid points). Figure 10 shows the resulting friction coefficients. For comparison, the friction coefficients as computed from the momentum balance at 1000 mb are also shown. The computed u friction coefficient compares favorably with observed u friction coefficient; in particular, note the structure and range. We do not emphasize exact matches in magnitude since the model can be tuned by altering the eddy viscosity or surface drag coefficient. The largest discrepancy is the positioning of the minimum α_u value, which is around 3°N in the computed, and at the equator in the observed. By comparison, the computed α_v does not compare well with observations. Both the positioning of the local minimum near the equator, as well as the range of the v friction values, is incorrect.

e. Importance of the boundary layer height

Why are the v friction coefficients computed from the model unsatisfactory? To examine how the friction coefficients are determined, we produce scatterplots in the Δp–R space the points involved in computing the u and v friction coefficients (Fig. 11). Note that the contours of friction coefficients vary more rapidly with Δp around $R \sim -1$ where the v friction points cluster, whereas between $-0.5 < R < 0$ (where the u friction points cluster) the variation in the friction coefficients arise primarily from variations in R. In other words,

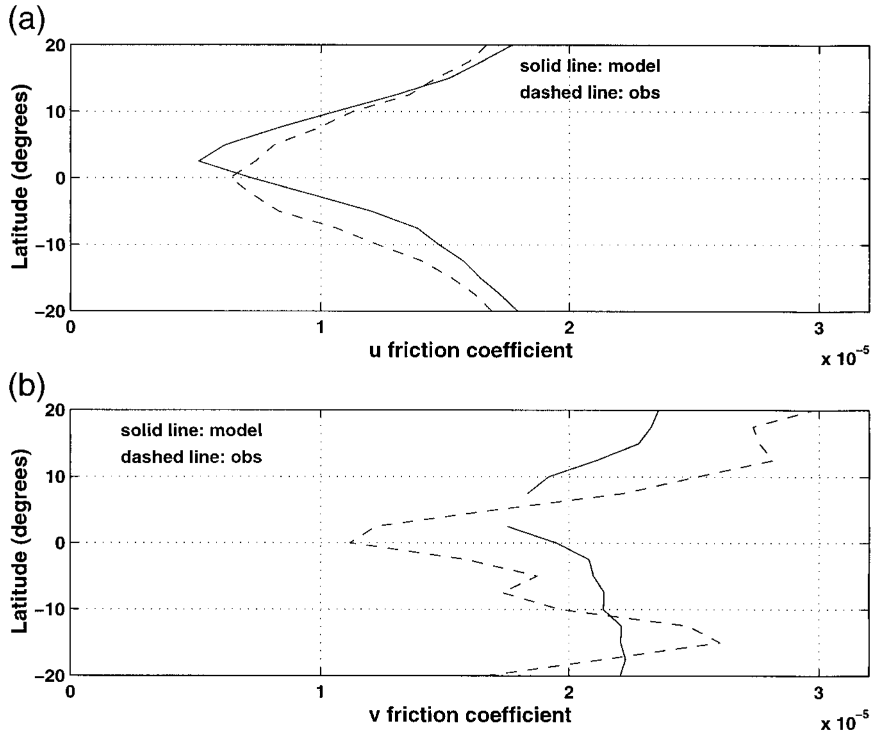

FIG. 10. (a) The u and (b) v friction coefficients computed from (13), using winds from NCEP reanalysis and PBL thickness derived from ISCCP D2 low cloud-top data. The missing part of the α_v curve corresponds to a region where surface $[v]$ is smaller than 0.1 m s^{-1} in absolute value. We mask this part out as (13) is sensitive errors in regions of small wind magnitudes. For comparison, the observed friction coefficients, computed from NCEP 1000-mb winds and geopotential, are also shown (dashed lines).

variations in α_v arise primarily from latitudinal variations in the imposed boundary layer height, whereas variations in α_u arise primarily from variations in R. This suggests the reason for lack of success in modeling α_v is due to incorrect specification of the PBL height. Here α_u is not affected by the same problem because zonal winds do not vary significantly near the top of the PBL (in the zonal mean they range between -5 and -3 m s^{-1}), and so the derived PBL top zonal winds are insensitive to the specification of PBL height. The derived R_u values are approximately correct, and hence the derived friction coefficients also.

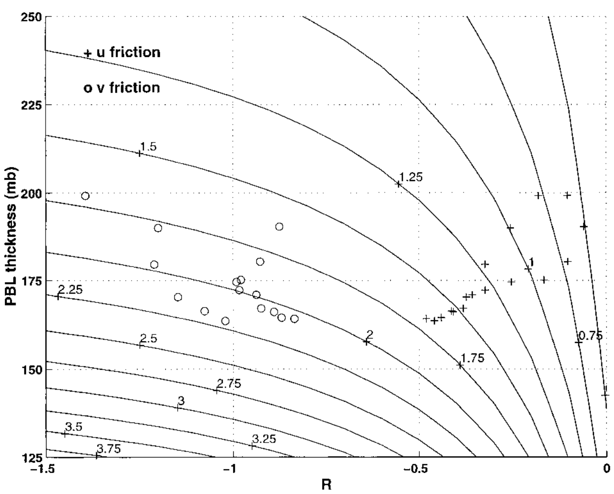

FIG. 11. Scatterplot of computed friction coefficients in Δp–R space. Circles are for α_v, and plus signs are for α_u. Contour lines represent values of the friction coefficient (in 10^{-5} s^{-1}) for given Δp and R.

4. Inverting the model to obtain boundary layer heights

a. Zonal-mean PBL height over the tropical Atlantic

The sensitivity of the meridional friction coefficient to boundary layer height presents an interesting way to obtain the boundary layer height from observed α_v. Since the v friction coefficient is relatively insensitive to R_v, we assume a fixed value of $R_v = -1$. This amounts to assuming that the meridional winds are small at the top relative to that at the surface, which is a good assumption. Here α_v then becomes purely a monotonic function of PBL thickness, and averaged climatological PBL height can thus easily be computed from the observed meridional friction coefficient.

Figure 12a shows PBL pressure heights computed from α_v derived from NCEP 1000-mb winds and geopotential heights over the tropical Atlantic for Northern Hemisphere summer (June–August). The derived PBL height (solid line of Fig. 12a) peaks at the ITCZ latitudes

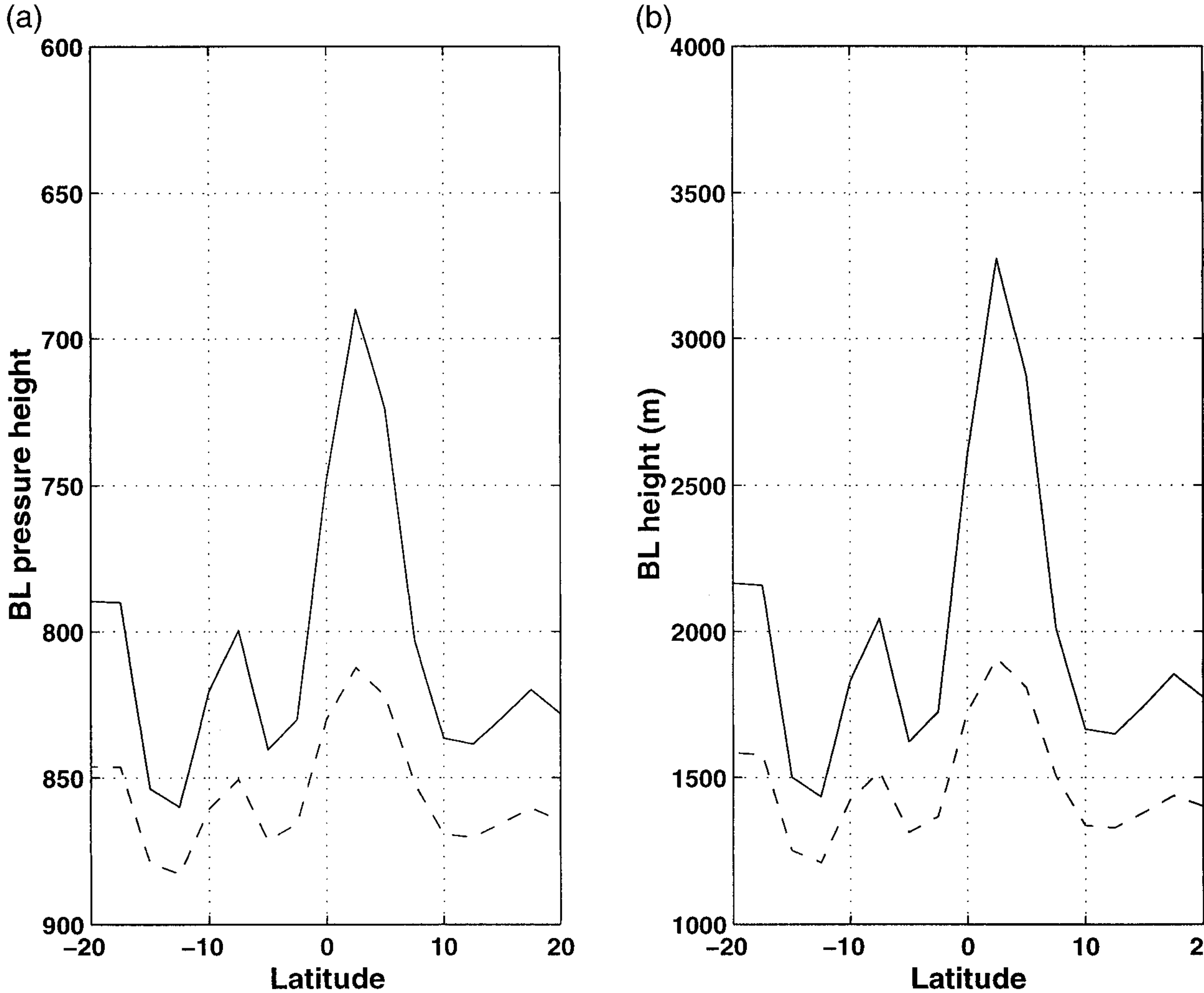

FIG. 12. Zonally averaged PBL heights derived from NCEP reanalysis α_v over the tropical Atlantic between Jun and Aug. (a) Pressure heights (mb), and (b) in m. The solid line is the height computed with the original NCEP α_v, and the dashed line is the height computed after adding a 1×10^{-5} s^{-1} offset to NCEP α_v.

around 3°N; away from the near Tropics, the height decreases to around the 830-mb level. To facilitate comparison with von Ficker's map of inversion heights (Fig. 9b), the PBL pressure heights are converted to meters (Fig. 12b, solid line). The structure of the derived PBL corresponds well with von Ficker's map: maximum inversion height at the equator and just north of it; and the lows just poleward north and south of the maximum. The derived PBL height even seems to capture the inversion height increases poleward of the lows (near 15°N/S). However, the magnitude of the heights is clearly too large: above 3000 m for the maximum in the derived PBL, compared to above 2000 m in von Ficker's map. We think the discrepancy in the magnitude is a result of the weak NCEP v friction coefficients; recall that the NCEP α_v is uniformly weaker than Da Silva α_v by about $\sim 1 \times 10^{-5}$ s^{-1} (section 2b). We recomputed PBL heights, applying this offset to NCEP α_v. The results (dashed lines in Fig. 12) show that the computed heights are clearly more realistic.

As mentioned earlier, there is some uncertainty with regards to the proper height scale for the PBL. It is of interest that the PBL height computed here—a calculation relying purely on surface information—bears resemblance to the inversion height.

b. Can we obtain full boundary layer heights?

It is tempting to apply the above method to obtain the full PBL height field. However, there are problems associated with the method for this application. First, while zonally averaged meridional winds above the PBL are small, the actual field itself may not be so. There may be significant meridional winds at the top of the PBL associated with land–sea contrast, or with orography. A good example is wind off the eastern coast of

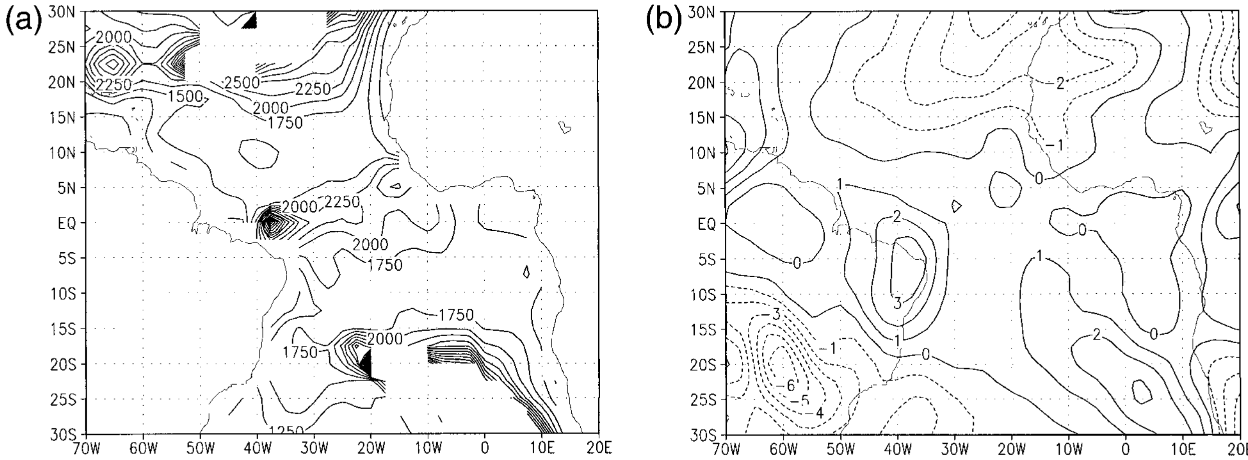

FIG. 13. (a) Computed PBL heights over the tropical Atlantic. Contour values are in meters. Blank regions over the ocean correspond to regions where the observed v friction coefficient is negative, for which there is no corresponding PBL height under the assumption that $R_v = -1$. (b) The 850-mb Jun–Aug climatological v wind, from the NCEP reanalysis. Contour values are in m s^{-1}.

Africa associated with the Indian monsoon. Hence, the assumption of small meridional winds above the PBL may not apply. Another problem is that, in computations, the residual term in the geostrophic balance is spatially very noisy, since geostrophy tends to work well to even within 5°–10° of the equator.

Nonetheless, it of interest to attempt such a calculation. We reduce the spatial noise problem by smoothing the individual terms in the momentum balance with a 1–2–1 filter, and we obtain v friction values over latitude and longitude by regressing the 12-month values of v and the residual of the v momentum geostrophic balance at each grid point. Figure 13a shows the result for the tropical Atlantic. The computed PBL heights capture the general pattern of deep PBL over the equatorial region, and lower PBL heights to the north and south of it. However, the PBL heights in the 10°N and 10°S region are too high—around 1500–1750 m, as opposed to 1250–1500 m according to von Ficker (Fig. 9b). Another major discrepancy is the lack of east–west gradients (low in east, high in west) in the subtropical PBL heights.

Why is the computed PBL height unrealistic? Figure 13b shows the reanalysis 850-mb meridional wind climatology over June–August. This shows that top of PBL meridional winds are not negligible compared to the surface meridional winds (approximately 3–7 m s^{-1}), as we had assumed. In general, factoring the upper-level winds into our analysis would increase R_v from -1 to somewhere between -1 and 0. For a given friction coefficient, the corresponding PBL height would be less than for the $R_v = -1$ case (see Fig. 8a). Hence, the inclusion of nonzero upper-level meridional winds would decrease the computed PBL heights in the subtropics, and more in line with observed heights. Note also that the upper-level winds tend to be stronger on the eastern sides of the Atlantic. It is possible that the east–west contrast in these winds may produce a more realistic east–west contrast in the computed PBL heights.

5. Summary and discussion

a. Summary

We diagnosed the monthly climatological surface momentum balance in a global surface marine dataset over the tropical oceans, assuming linear friction. In agreement with Deser (1993), we find that the friction coefficient for v is two to three times larger than the u friction coefficient. Also, in agreement with Li and Wang (1994), and Kushnir and Kaplan (1994), we find a systematic meridional dependence in both friction coefficients. Both friction coefficients are seen to be increasing roughly symmetrically away from the equator, up to around 20°N and 20°S. The v friction coefficient increases faster than the u friction coefficient. We find that, to first approximation, the friction coefficient is independent of longitude and season, in the tropical band between 20°S and 20°N. Poleward of this tropical band, the correlation between the residual of the momentum balance and the components of the wind magnitude degrade substantially, implying that the friction coefficient has zonal and/or seasonal dependence. We also found this qualitative behavior in the NCEP reanalysis 1000-mb winds, although the NCEP α_v is approximately uniformly weaker than the Da Silva α_v by about 1×10^{-5} s^{-1}.

Following Deser's (1993) suggestion, we modeled the friction coefficients using a K-theory Ekman layer with constant viscosity. The vertical structure of the boundary layer was decomposed into eigenfunctions of the vertical diffusion operator, assuming a stress proportional to the wind speed at the surface, and a flux ratio condition at the top of the boundary layer. We then simplified the vertical structure by assuming that the boundary layer can be adequately represented by a combination of the two gravest vertical modes. We rederived the expression for the surface momentum balance, but with an explicit expression for the friction coefficients as a function of the PBL thickness, and the ratio of the $j = 1$ to $j = 0$ amplitudes. This ratio can be found from knowing the wind magnitudes at the surface and top of the PBL. For characteristic PBL thickness (around 150 mb) and typical u and v profiles found in the tropical PBL, the magnitudes of the friction coefficients calculated are found to be comparable to those found from diagnosis of the surface momentum balance.

We tested the model further by computing the friction coefficients using NCEP reanalysis data, and using PBL heights derived from ISCCP D2 low cloud-top temperatures and the assumption of a constant (5.2 K km^{-1}) lapse rate. Applying our model, we found that the u friction coefficient compared well with observations in both structure and magnitude, but the structure of the derived v friction coefficient did not compare at all well with observations. We found that the v friction calculation was sensitive to the specification of boundary layer height, and the lack of agreement between model and observations was attributed to inaccuracies in the PBL thickness values used.

The assumption of a small zonal-mean meridional wind component at the top of the boundary layer allowed an inverse calculation to obtain zonally averaged PBL heights from the observed v friction coefficients. We applied this technique, using observed NCEP α_v, over the tropical Atlantic for the Northern Hemisphere summer (June–August). The structure of PBL heights thus produced compared favorably with observed inversion heights, though the magnitude was too large. We showed that the discrepancy in magnitude could be accounted for by adding in the observed $\sim 1 \times 10^{-5}$ s^{-1} offset between NCEP and Da Silva v friction coefficients. The same technique applied to obtain the full two-dimensional PBL height field was less successful. This failure was attributed to the assumption of negligible meridional winds at the top of the PBL. While this assumption holds well for the zonally averaged v, it is a poor assumption for the full v wind field.

b. Discussion

We started our modeling analysis by posing these questions:

- Why is $\alpha_u < \alpha_v$?
- Why do both α_u and α_v increase with latitude away from the equator?
- Why does α_v increase faster than α_u?

We suggest the following answers from analysis of our model.

- Here $\alpha_u < \alpha_v$ *is a consequence of the asymmetry in wind strength at the top of the PBL diffusing down to the surface.* This is the mechanism that Deser (1993) suggested. More specifically, meridional wind at the top of the PBL is typically negligible, whereas zonal wind at the top of the PBL is comparable in magnitude and of the same sign as the surface zonal wind. For the surface zonal momentum balance, there is a contribution from momentum mixing from above that counteracts the retarding surface fluxes. No such mechanism operates for surface meridional wind.
- *The increase for both* α_u *and* α_v *is a consequence of the decreasing thickness of the PBL with latitude away from the equator.* Mathematically, a smaller PBL thickness implies that, all else being the same, the vertical curvature of the wind profile is larger and hence so will be the friction coefficient. Physically, we understand this to mean that the momentum flux from the surface distributes itself over a thinner layer, and hence the retardation of wind in the PBL is stronger.
- *The faster increase in* α_v *relative to* α_u *is a consequence of the different vertical profiles of* u *and* v*, and how they react to changing boundary layer thickness.* We showed this mathematically in Fig. 8b, where the $R = -1$ friction coefficient changed faster than the $R = -0.15$ coefficient with changing PBL thickness. It is difficult to interpret this physically, and we offer only a partial interpretation. A smaller PBL thickness increases friction, as we have argued above. However, it also means that the strong PBL top zonal winds are closer to the surface, and thus more able to influence the surface zonal wind balance. Consequently, the increase in α_u caused by decreasing PBL thickness is moderated.

Our results suggest that PBL height is an important component in modeling tropical surface winds. Models traditionally underestimate surface meridional wind, producing surface wind fields that are too zonal. This trait is also recognized in simple models of the tropical atmosphere (Zebiak 1982 and 1986; Neelin 1988; Seager 1991; Wang and Li 1993). However, this property of simple models is at odds with what observations might suggest. As those models use the same linear friction coefficient for both u and v, and are tuned to give good zonal wind simulations (as they are more important for ENSO studies), the friction applied to the meridional wind should be too small. Hence, one might expect the opposite of what these models actually obtain: that meridional winds should be too strong in simple model simulations. The implication is that simple models are producing incorrect pressure gradient fields. They are likely producing better simulations of the winds at the upper levels of the PBL, where the zonal winds are stronger and the meridional winds less so. This suggests that surface wind simulations can be vastly improved in these simple ''Gill-type'' models by the addition of an Ekman-type PBL (cf. Chiang and Zebiak 1998).

While knowing that different and meridionally varying u and v linear friction coefficients exists is important for applications of the balance to simple modeling and data assimilation problems, left alone it is quite unsatisfactory. The meridional structure in the linear friction coefficients implies that there is information in the residual of the geostrophic balance that is not adequately being exploited. A different but still relatively simple parameterization of friction might be able to improve the steady surface momentum balance. Our results suggest that the PBL top winds and thickness are essential inputs to any improvement of PBL friction parameterization.

Acknowledgments. JCHC thanks Alexey Kaplan for his advice and his encouragement of this work. Mark Cane gave valuable comments and advice on an earlier version of this paper. We also thank Richard Seager, Yochanan Kushnir, Mike Evans, Martin Visbeck, and two anonymous reviewers for useful comments and suggestions. The input of Alan Betts, Patrick Minnis, and Steve Esbensen is gratefully acknowledged for deriving the PBL height from low cloud-top temperatures. This work is supported by a NASA Earth Systems Science Fellowship (to JCHC), and NSF Grant ATM 92-24915 (to SEZ). This is Lamont-Doherty Earth Observatory Contribution Number 5967.

REFERENCES

Augstein, E., H. Riehl, F. Ostapoff, and V. Wagner, 1973: Mass and energy transports in an undisturbed Atlantic trade-wind flow. *Mon. Wea. Rev.,* **101,** 101–111.

——, H. Schmidt, and F. Ostapoff, 1974: The vertical structure of the atmospheric planetary boundary layer in undisturbed trade winds over the Atlantic Ocean. *Bound.-Layer Meteor.,* **6,** 129–150.

Betts, A. K., P. Minnis, W. Ridgeway, and D. F. Young, 1992: Integration of satellite and surface data using a radiative–convective oceanic boundary-layer model. *J. Appl. Meteor.,* **31,** 340–350.

Cardone, V. J., J. G. Greenwood, and M. A. Cane, 1990: On trends in historical marine wind data. *J. Climate,* **3,** 113–127.

Chertock, B., C. W. Fairall, and A. B. White, 1993: Surface-based measurements and satellite retrievals of broken cloud properties in the equatorial Pacific. *J. Geophys. Res.,* **98,** 18 489–18 500.

Chiang, J. C. H., and S. E. Zebiak, 1998: Modeling surface winds over tropical oceans: Effect of a simple diffusive boundary layer on convectively forced anomalous winds. *Proc. 23d Climate Diagnostics and Prediction Workshop,* Miami, FL, U.S. Department of Commerce, Springfield, VA, 95–98.

Da Silva, A. M., C. C. Young, and S. Levitus, 1994: *Atlas of Surface Marine Data 1994.* Vol. 1, *Algorithms and Procedures.* U.S. Department of Commerce, National Oceanic and Atmospheric Administration, 83 pp.

Deardorff, J. W., 1972: Parameterization of the planetary boundary layer for use in general circulation models. *Mon. Wea. Rev.,* **100,** 93–106

Deser, C., 1993: Diagnosis of the surface momentum balance over the tropical Pacific Ocean. *J. Climate,* **6,** 64–74.

Hastenrath, S., 1991: *Climate Dynamics of the Tropics.* Kluwer Academic Publishers, 488 pp.

Holland, J. Z., and E. M. Rasmusson, 1973: Measurements of the atmospheric mass, energy, and momentum budgets over a 500-kilometer square of tropical ocean. *Mon. Wea. Rev.,* **101,** 44–55.

Kalnay, E., and Coauthors, 1996: The NCEP/NCAR 40-Year Reanalysis Project. *Bull. Amer. Meteor. Soc.,* **77,** 437–471.

Klein, S. A., and D.L. Hartmann, 1993: The seasonal cycle of low stratiform clouds. *J. Climate,* **6,** 1587–1606.

Kloesel, K. A., and B. A. Albrecht, 1989: Low-level inversions over the tropical Pacific—Thermodynamic structure of the boundary layer and the above-inversion moisture structure. *Mon. Wea. Rev.,* **117,** 87–101.

Kushnir, Y., and A. Kaplan, 1994: Dynamical constraints for the analysis of sea level pressure and surface wind over the World Ocean. *Proc. Int. COADS Wind Workshop,* Kiel, Germany, U.S. Department of Commerce, 91–101.

Li, T., and B. Wang, 1994: A thermodynamic equilibrium climate model for monthly mean surface winds and precipitation over the tropical Pacific. *J. Climate,* **51,** 1372–1385.

Minnis, P., P. W. Heck, D. F. Young, C. W. Fairall, and J. B. Snider, 1992: Stratocumulus cloud properties derived from simultaneous satellite and island-based instrumentation during FIRE. *J. Appl. Meteor.,* **31,** 317–339.

Murphree, T., and H. van den Dool, 1988: Calculating winds from time mean sea level pressure fields. *J. Atmos. Sci.,* **45,** 3269–3281.

Neelin, J. D., 1988: A simple model for surface stress and low-level flow in the tropical atmosphere driven by prescribed heating. *Quart. J. Roy. Meteor. Soc.,* **114,** 747–770.

Riehl, H., T. C. Yeh, J. S. Malkus, and N. A. LaSeur, 1951: The north-east trade of the Pacific Ocean. *Quart. J. Roy. Meteor. Soc.,* **77,** 598–626.

Rossow, W. B., A. W. Walker, D. E. Beuschel, and M. D. Roiter, 1996: International satellite cloud climatology project (ISCCP) documentation of new cloud datasets. Tech. Doc. WMO/TD-No. 737, WMO, 55 pp.

Seager, R., 1991: A simple model of the climatology and variability of the low-level wind field in the Tropics. *J. Climate,* **4,** 164–179.

Schubert, W. H., P. E. Ciesielski, C. Lu, and R. H. Johnson, 1995: Dynamical adjustment of the trade-wind inversion layer. *J. Atmos. Sci.,* **52,** 2941–2952

Stout, J. E., and J. A. Young, 1983: Low-level monsoon dynamics derived from satellite winds. *Mon. Wea. Rev.,* **111,** 774–798.

Stull, R. B., 1988: *An Introduction to Boundary Layer Meteorology.* Kluwer Academic Publishers, 666 pp.

von Ficker, H., 1936: Die Passatinversion. *Veroeff. Meteor. Inst. Univ. Berlin,* **1,** 1–33.

Wallace, J. M., T. P. Mitchell, and C. Deser, 1989: The influence of sea surface temperature on surface wind in the eastern equatorial Pacific: Seasonal and interannual variability. *J. Climate,* **2,** 1492–1499

Wang, B., and T. Li, 1993: A simple tropical atmosphere model of relevance to short-term climate variations. *J. Atmos. Sci.,* **50,** 260–284.

Young, J. A., 1987: Boundary layer dynamics of tropical and monsoonal flows. *Monsoon Meteorology,* C.-P. Chang and T. N. Krishnamurty, Eds., Oxford University Press, 461–500.

Zebiak, S. E., 1982: A simple atmospheric model of relevance to El Niño. *J. Atmos. Sci.,* **39,** 2017–2027.

——, 1986: Atmospheric convergence feedback in a simple model for El Niño. *Mon. Wea. Rev.,* **114,** 1263–1271.

——, 1990: Diagnostic studies of Pacific surface winds. *J. Climate,* **3,** 1016–1031.